Received: 10 April 2016 Revised: 28 July 2016 Accepted: 6 August 2016

(wileyonlinelibrary.com) DOI 10.1002/xrs.2708

Assessing silicon deposits in Zilfi province, Saudi Arabia, using XRF and XRD techniques

Atta G. Attaelmanan,[a]* Nawal M. Suleman,[b] Ibrahim A. El Agib[c] and Hamed A Al-Sewaidan[c]

The aim of this project is to create a geochemical database of the Nafud Desert in Zilfi Province, which lies 260 km northwest of Riyadh, capital of Saudi Arabia, and assess its potential as a silicon mine. The area of study was surveyed during December 2012 collecting 21 geological samples from 7 places (Alsabla, Almatal, Shlwan, Alaaga, Jaway, Magra and Althuare).

Elemental composition was determined using X-ray fluorescence spectrometry, while mineral content and crystallography analysis was performed using X-ray diffraction.

Analysis results revealed that silicon was abundant in the area, in fairly homogeneous amounts. Silica was found in concentrations of around 93% per sampled mass, and silicon concentrations were around 42%, in the surface layers down to the depth of 40 cm.

Other elements (Al, K, Ca, Ti, Cr, Mn, Fe, Sr, Zr and Pd) were present in very low concentrations, except for aluminium oxide, which was present in three areas (Jaway, Magra and Althuare) at concentrations around 5%, while Alsabla samples showed higher concentrations of CaO. Thus, according to the results, the Nafud Desert is a rich source of silicon that can be exploited very cheaply because of the presence of the raw material on the surface.

Introduction

Silicon (Si) is one of the most abundant elements in the continental crust and consequently is utilized in many industries extending from house hold items to advanced technologies.[1–4] However, silicon metal demand comes predominately from the aluminium and chemical industries, with more than 75% of silicon metal produced worldwide, is normally used by the chemical industry.

In Saudi Arabia, the production and demand for silicon is expected to rise because of to the expansion of the existing companies operating in the minerals sector. Furthermore, Saudi Arabia is best positioned to attract silicon ingot/wafer projects because of many favourable reasons including the relatively inexpensive energy resources, spacious and flexible production plots, and local glass production.[5]

Assessment of mineral deposits are usually conducted via physical and chemical analysis of geological samples using techniques such as inductively coupled plasma-mass spectrometry (ICP-MS),[6–8] emission and atomic absorption spectrometry[9] and neutron activation analysis (NAA).[10] X-ray fluorescence (XRF) and X-ray diffraction (XRD) are two of the most utilized techniques for the determination of elemental and chemical composition of such samples.[11,12] XRF has the advantage of minimum sample preparation and high-detection sensitivity for a wide range of elements extending from sodium to uranium, with great accuracy,[13] while XRD offers the possibility of identifying the crystal structure of the chemical compounds present in the sample.[14]

The aim of this project is to advance current research attempting to create a geochemical database of the studied area, which would be useful for assessing the potential of the area as a silicon mine, and to aid future explorations.

Material and methods

Nafud Desert in Zilfi province, which lies 260 km northwest of Riyadh, the capital of Saudi Arabia. The area of study was surveyed during December 2012 collecting 21 geological samples (100 g each) from seven places (Alsabla, Almatal, Shlwan, Alaaga, Jaway, Magra and Althuare), by collecting three samples from each place: at the surface, 20 cm and 40 cm depths. To ensure good representation, samples were first sieved using a 200 mm sieve and then mixed thoroughly before being milled using a mortar and pestle.

All the samples were analyzed using an X-ray Analytical Microscope (XGT 7200, Horiba, Japan)[15] operating with a rhodium (Rh) X-ray tube and an energy dispersive, peltier cooled silicon drift detector, capable of detecting elements from sodium (Na) to uranium (U). Operational conditions were: 50 kV tube's high voltage, 0.5 mA tube current, and 1000 s per point analysis time. A mono glass capillary is utilized to generate a 1.2 mm X-ray spot on the surface of the sample. Analysis was conducted under vacuum to improve the detection sensitivity of light elements. Elemental composition was determined for oxides as mass percentages.

---

* *Correspondence to: Atta G. Attaelmanan, University of Sharjah, Sharjah, United Arab Emirates. E-mail: aattaelmanan@sharjah.ac.ae*

a *University of Sharjah, Sharjah, United Arab Emirates*

b *Majmaah University, Riyadh, Saudi Arabia*

c *King Saud University, Riyadh, Saudi Arabia*

X-ray diffraction analysis was performed on the powder samples using an XRD system (8D-Advance, Bruker Instruments, Germany). Spectra were collected using Cu X-ay tube with a nickel filter generating Kα photons of energy 8.04 keV and wavelength 1.5418 Å, with the tube current set at 40 mA. Scan settings were from $2\theta = 18^{\circ}$ to 83° with an increment of 0.02°. Total scan time was 1664 s, at 0.5 s per reading.

Results and discussion

X-ray fluorescence analysis revealed that all the samples show high concentrations of silica (SiO_2) ranging between 85% and 98% per mass content, with an average value of approximately 93% (table 1). In addition to silicon, other elements were detected in low concentrations such as Al, K, Ca, Mn and Fe, while Ti, Cr, Sr, Zr and Pd are present in trace amounts close to the detection limits (table 2). All the elements showed a rather homogeneous spatial distribution, except for Al_2O_3, which was present in three areas only (Alaaga, Jaway and Magra) in concentrations of around 5%, and CaO was present in two of Alsabla samples in concentrations of around 8%, which are higher than in the other samples. Potassium and iron concentrations were in average around 1% and 2% consecutively, in most of the samples.

Table 3 lists the concentration of silicon in the collected samples. As shown, Si concentrations are between 40% and 45%, which are consistent with results of ICP-MS analysis conducted on the same samples by Suleman and El Agib,[16] which reported Si concentrations between 42.8% and 44.9%. The error values in the XRF data are 3σ, which indicates a 99.73% confidence in the measured values.

The small variations between the XRF and ICP-MS results are most probably due to variations in the sampling process and the sensitivity of both techniques to the detection of Si. In both cases a few grams are selected as representatives of the bulk samples collected, and thus variations would exist despite the homogenizations processes employed. The two techniques also differ in sample preparation and that might account for results' differences. ICP-MS samples are turned into solutions using appropriate reagents, while XRF samples need no sample preparation and are analyzed in their original solid powder form. Similar to the ICP-MS technique, the XGT-7200 X-ray microscope employed here offers high detection sensitivity for elements above Na and very low detection limits, which is reflected in the small error values compared to those reported by the ICP-MS results. Moreover, during the actual analysis by both techniques, only a tiny volume is sampled either as a few millilitres of solution in the case of ICP-MS, or in XRF by a few micrograms defined by the 1.2 mm X-ray beam. However, all the effects of these factors were minimized by the sieving, homogenizing and milling processes.

No major variations were detected in the elemental composition at different depths. However some samples showed variations between the Si concentrations in the different layers. These variations are due to the presence of other elements such as K, Ca and Fe in higher concentrations in some layers and their absence from others. For example, in the three Alsabla samples, SiO_2 concentrations varied across the three layers such that they were 90.48%, 93.78% and 84.97 at the top, and 20- and 40-cm layers, respectively. Inspection of the other elements present in the three layers reveals that CaO was high in the top layer at 7.08%, and at 40-cm depth, it was 9.96%, while only 1.62% in the 20-cm layer. Also, Fe_2O_3 was present in considerable concentrations (1.76%, 2.88% and 3.92%), which lead to the considerable variations in Si concentrations. Figure 1 shows an example of the XRF spectra from the three samples collected at Alaaga.

XRD analysis revealed that the major crystals forming the sand material is silicon oxide either as quartz (SiO_2) arranged in hexagonal lattice structure (a = 4.91 Å, b = 4.91 Å and c = 5.41 Å), or quartz-alpha Fe-doped brown (α-SiO_2) arranged in triclinic lattice structure (a = 4.91 Å, b = 4.92 Å and c = 5.41 Å). Figure 2 shows the XRD spectra from seven samples collected at 40 cm below the surface.

Table 1. Concentrations of the major elements shown as mass% ± 3σ

Sampling site	Al_2O_3	SiO_2	K_2O	CaO	TiO_2	Fe_2O_3
Alsabla at surface	—	90.48 ± 0.05	—	7.08 ± 0.06	0.24 ± 0.02	1.76 ± 0.02
Alsabla (20-cm depth)	—	93.78 ± 0.04	1.18 ± 0.04	1.62 ± 0.03	0.22 ± 0.01	2.88 ± 0.02
Alsabla (40-cm depth)	—	84.97 ± 0.14	—	9.96 ± 0.09	0.6 ± 0.02	3.92 ± 0.03
Almatal at surface	—	93.8 ± 0.05	2.14 ± 0.06	0.51 ± 0.03	0.3 ± 0.02	2.67 ± 0.02
Almatal (20-cm depth)	—	97.96 ± 0.03	0.43 ± 0.02	0.21 ± 0.01	0.11 ± 0.01	0.75 ± 0.01
Almatal (40-cm depth)	—	94.98 ± 0.05	1.98 ± 0.04	0.39 ± 0.02	0.16 ± 0.01	1.25 ± 0.01
Shlwan at surface	—	95.15 ± 0.03	1.96 ± 0.04	0.76 ± 0.02	0.4 ± 0.02	1.51 ± 0.01
Shlwan (20-cm depth)	—	96.86 ± 0.03	0.74 ± 0.03	0.63 ± 0.02	0.14 ± 0.01	1.01 ± 0.01
Shlwan (40-cm depth)	—	96.64 ± 0.03	—	1.77 ± 0.02	0.12 ± 0.01	1.09 ± 0.01
Alaaga at surface	—	95.47 ± 0.04	1.74 ± 0.04	0.51 ± 0.03	0.27 ± 0.02	1.75 ± 0.02
Alaaga (20-cm depth)	5.38 ± 0.08	92.04 ± 0.09	0.89 ± 0.03	0.33 ± 0.02	0.16 ± 0.01	1.03 ± 0.01
Alaaga (40-cm depth)	5.98 ± 0.09	91.42 ± 0.010	0.85 ± 0.02	0.51 ± 0.02	0.15 ± 0.01	0.87 ± 0.01
Jaway at surface	4.59 ± 0.08	93.77 ± 0.07	0.42 ± 0.02	0.22 ± 0.01	0.12 ± 0.01	0.77 ± 0.01
Jaway (20-cm depth)	5.59 ± 0.08	91.77 ± 0.08	0.96 ± 0.03	0.45 ± 0.02	0.2 ± 0.01	0.9 ± 0.01
Jaway (40-cm depth)	6.24 ± 0.09	90.09 ± 0.08	2.03 ± 0.03	0.42 ± 0.02	0.14 ± 001	0.92 ± 0.01
Magra at surface	6.69 ± 0.11	89.42 ± 0.09	1.28 ± 0.03	0.72 ± 0.02	0.24 ± 0.01	1.44 ± 0.01
Magra (20-cm depth)	6.36 ± 0.09	89.14 ± 0.08	2.07 ± 0.04	0.91 ± 0.02	0.16 ± 0.01	1.15 ± 0.01
Magra (40-cm depth)	4.77 ± 0.09	93.35 ± 0.08	0.41 ± 0.02	0.26 ± 0.02	0.14 ± 0.01	0.87 ± 0.01
Althuare at surface	5.63 ± 0.1	87.4 ± 0.09	1.26 ± 0.03	2 ± 0.03	0.55 ± 0.01	2.05 ± 0.01
Althuare (20-cm depth)	—	96.16 ± 0.03	0.94 ± 0.02	0.93 ± 0.02	0.33 ± 0.01	1.39 ± 0.01
Althuare (40-cm depth)	0.37 ± 0.05	96.84 ± 0.06	0.41 ± 0.02	0.75 ± 0.02	—	0.73 ± 0.01

Table 2. Concentrations of the trace elements shown as mass% ± 3σ

Sampling site	Cr_2O_3	MnO_2	SrO	ZrO_2	PdO
Alsabla at surface	0.03 + 0.01	0.11 ± 0.01	0.02 + 0.00	0.13 ± 0.00	0.04 ± 0.01
Alsabla (20-cm depth)	0.11 ± 0.01	0.03	0.02 ± 0.00	0.05 ± 0.00	0.04 ± 0.01
Alsabla (40-cm depth)	0.11 ± 0.02	—	0.05 ± 0.01	0.1 ± 0.00	0.05 ± 0.02
Almatal at surface	0.08 ± 0.01	0.09 ± 0.01	0.03 ± 0.00	0.18 ± 0.00	0.06 ± 0.01
Almatal (20-cm depth)	0.02 ± 0.01	—	0.01 ± 0.00	0	0.02 ± 0.01
Almatal (40-cm depth)	0	0.05 ± 0.01	0.02 ± 0.00	0.1 ± 0.00	0.05 ± 0.01
Shlwan at surface	0.05 ± 0.01	0.03 ± 0.01	0.03 + 0.00	0.05 ± 0.00	0.04 ± 0.01
Shlwan (20-cm depth)	0.09 ± 0.01	0.04 ± 0.01	0.02 ± 0.00	0.01 ± 0.00	0.03 ± 0.01
Shlwan (40-cm depth)	—	—	0.02 ± 0.00	0.02 ± 0.00	0.03 ± 0.01
Alaaga at surface	0.04 ± 0.01	—	0.03 ± 0.00	0.02 ± 0.00	0.05 ± 0.01
Alaaga (20-cm depth)	—	—	0.02 ± 0.00	0.1 ± 0.00	0.02 ± 0.01
Alaaga (40-cm depth)	0.050.01	0	0.02 ± 0.00	0.11 ± 0.00	0.02 ± 0.01
Jaway at surface	0.01 ± 0.00	0.02 ± 0.00	0.01 ± 0.00	0.04 ± 0.00	0.01 ± 0.01
Jaway (20-cm depth)	0.02 ± 0.00	—	0.02 ± 0.00	0.06 ± 0.00	0.02 ± 0.01
Jaway (40-cm depth)	0.02 ± 0.01	0.01 ± 0.00	0.01 ± 0.00	0.05 ± 0.00	0.0 ± 0.01
Magra at surface	0.02 ± 0.01	0.01 ± 0.00	0.02 ± 0.00	0.11 ± 0.00	0.03 ± 0.01
Magra (20-cm depth)	—	0.02 ± 0.00	0.02 ± 0.00	0.04 ± 0.00	0.03 ± 0.01
Magra (40-cm depth)	0.03 ± 0.00	0	0.01 ± 0.00	0.02 ± 0.00	0.02 ± 0.01
Althuare at surface	0.05 ± 0.01	0.04 ± 0.00	0.03 ± 0.00	0.44 ± 0.00	0.04 ± 0.01
Althuare (20-cm depth)	0.01 ± 0.00	0.01 ± 0.00	0.02 ± 0.00	0.13 ± 0.00	0.01 ± 0.00
Althuare(40-cm depth)	0.02 ± 0.01	—	0.01 ± 0.00	0.03 ± 0.00	0.02 ± 0.01

Table 3. Silicon concentrations reported as mass% ± 3σ. Values in brackets are the inactively coupled plasma-mass spectrometry results

	Surface	20 cm below surface	40 cm below surface
Alsabla	42.30 ± 0.05 (43.3 ± 0.4)	43.84 ± 0.04 (43.8 ± 0.5)	39.72 ± 0.13 (43.5 ± 0.9)
Almatal	43.85 ± 0.05 (44.0 ± 0.6)	45.79 ± 0.03 (44.1 ± 0.8)	44.40 ± 0.05 (43.9 ± 0.9)
Shalwan	44.48 ± 0.03 (44.3 ± 0.9)	45.28 ± 0.03 (44.2 ± 1.0)	45.17 ± 0.07 (43.8 ± 0.5)
Alaaga	44.63 ± 0.04 (43.9 ± 0.9)	43.03 ± 0.08 (44.3 ± 0.9)	42.73 ± 0.08 (44.2 ± 0.4)
Jaway	43.83 ± 0.07 (43.8 ± 1.0)	42.90 ± 0.08 (44.6 ± 1.0)	42.11 ± 0.08 (43.7 ± 1.0)
Magra	41.80 ± 0.09 (42.8 ± 0.4)	41.67 ± 0.08 (44.9 ± 0.8)	43.64 ± 0.08 (43.9 ± 1.0)
Althuare	40.86 ± 0.09 (44.5 ± 1.6)	44.95 ± 0.03 (43.8 ± 0.6)	45.27 ± 0.06 (44.0 ± 0.7)

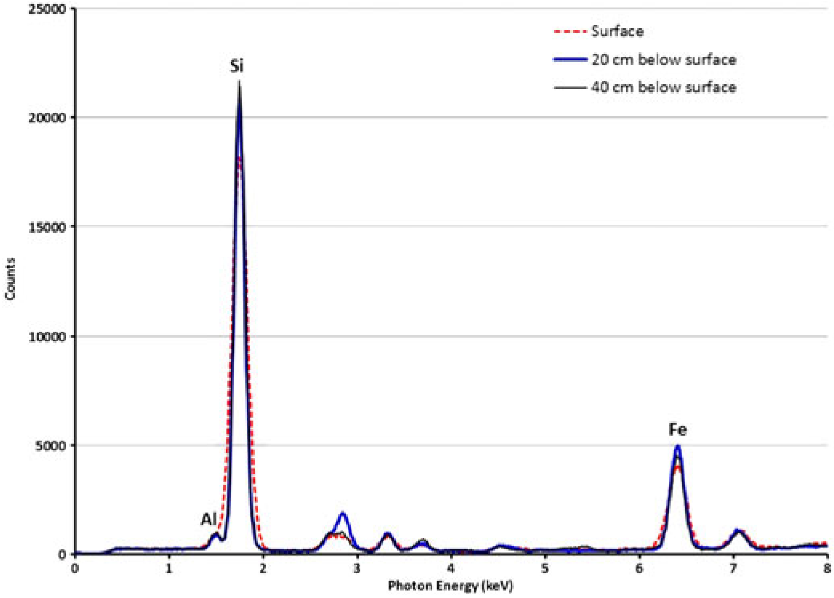

Figure 1. X-ray fluorescence spectra from Alaaga's three samples, showing very small variations.

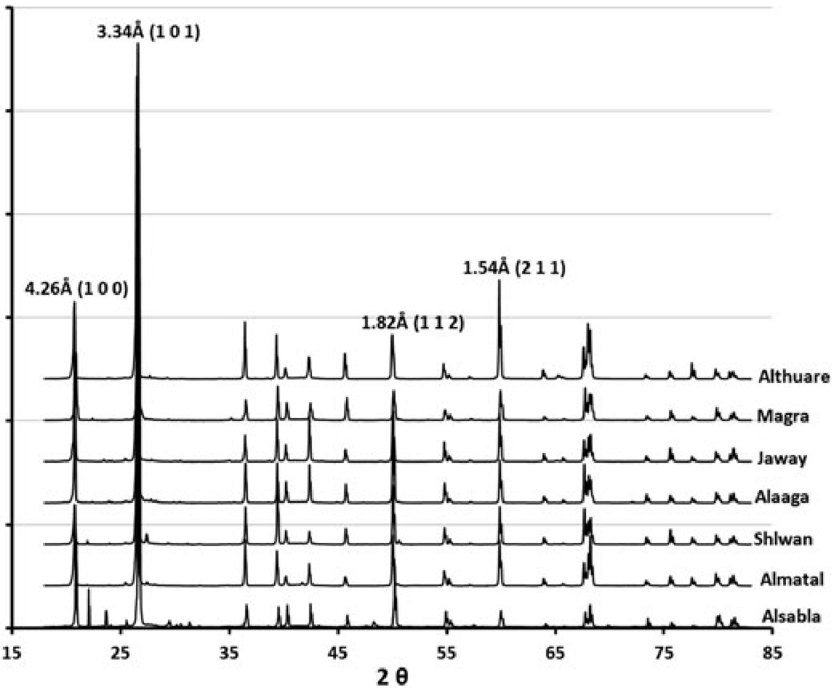

Figure 2. XRD spectra for samples collected at 40 cm below surface at the seven locations. Miller indices and d-pacing values are shown for the four major peaks.

The stacked spectra show the major and minor diffraction peaks representing different crystal planes. Some of the peaks are identified according to their d-spacing and Miller indices values, where the most prominent plane has Miller indices of (1 0 1). It is clear from the spectra that the samples are very similar in their mineral compositions.

Conclusions

It is evident from the analytical results that silicon, in the form of silica (SiO_2), is present in abundance in the surveyed areas in Nafud Desert. Silica was found in concentrations of around 93% per sampled mass, and silicon concentrations were around 42%, in the surface layers down to the depth of 40 cm. Results obtained in this investigation via XRF analysis are comparable to results obtained via ICP-MS.

Other elements (Al, K, Ca, Mn, Fe) were present in very low concentrations, except for aluminium oxide, which was present in three areas (Jaway, Magra and Althuare) at concentrations around 5%, while Alsabla samples showed higher concentrations of CaO. The presence of these impurities can alter the colour, chemical, optical and mechanical properties of any end product,[17,18] that is why it is imperative to identify and quantify them.

Thus, according to the results, the Nafud Desert is a rich source of silicon that can be exploited very cheaply because of the presence of the raw material on the surface, with expected returns of around 400 kg of pure silicon per 1 ton of processed sand. Moreover, no appreciable differences of silica concentrations were detected at different depths.

Acknowledgements

The authors gratefully thank Majmaah University for their financial support and the dean of Scientific Research, Majmaah University.

Analysis was performed at the Advanced Materials Research Centre, University of Sharjah.

References

[1] F. K. Lutgens, E. J. Tarbuck, *Essentials of Geology*, 9th edn, Prentice Hall, Upper Saddle River, NJ, **2006**.
[2] V. Lindroos, M. Tilli, A. Lehto, T. Motooka, *Handbook of Silicon Based MEMS Materials & Technologies*, William Andrew Applied Science Publishers, Norwich, **2010**.
[3] J. D. Cressler, *Silicon Earth: Introduction to the Microelectronics and Nanotechnology Revolution*, Cambridge University Press, Cambridge, **2009**.
[4] U.S. Geolgical Survey **2015**. Mineral Commodity Summaries.
[5] The KICP Annual Strategic Study **2009**, "Saudi Arabia Solar Energy: Manufacturing and Technology, Assessment". p.14
[6] H. Uchida, T. Uchida, C. Lida. Determination of minor and trace elements in silicate rocks by inductively coupled plasma emission spectrometry. *Anal. Chim. Acta* **1980**, *116*, 433–436. doi:10.1016/S0003-2670(01)95228-6.
[7] S. Hauptkorn, V. Krivan, B. Gercken, J. Pavel. Determination of trace impurities in high purity quartz by electrochemical vaporization ICP mass spectrometry using slurry sampling technique. *J. Anal. At. Spectrom.* **1997**, *12*, 421–428. doi:10.1039/a606027g.
[8] M. S. Szeto, J. H. L. Opdebeeck, J. C. Vanloon, J. Kreins. Determination of Fe in silica sand, nepheline 0syanite and feldspar samples. *At. Spectrosc.* **1984**, *5*, 186–188.
[9] K. Dash, K. Chandrasekaran, S. Thangavel, S. M. Dhaville, J. Arunachalam. Determination of trace metallic impurities in high purity quartz by ion chromatography. *J. Chromatogr. Acta.* **2004**, *1022*, 25–31. doi:10.1016/j.chroma.2003.08.014.
[10] B. E. Kogo, E. N. Gajere, J. K. Ogunmola, J. O. Ogbole. Neutron activation analysis of soil samples from different parts of abuja metropolis. *Middle-East J. Sci. Res.* **2009**, *4*(4), 254–262.
[11] V. Singh, H. M. Agrawal. Qualitative soil mineral analysis by EDXRF, XRD and AAS probes. *Radiat. Phys. Chem.* **2012**, *81*, 1796–1803.
[12] A. G. Attaelmanan. Identification of mineral inclusions in Archaeological ceramics using microbeam X-ray spectrometry. *X-ray spectrom.* **2014**, *43*(6), 325–331.
[13] A. Attaelmanan, S. Larsson, A. Rindby, P. Voglis, A. Kuczumow. A table-top microbeam scanning facility. *Rev. Sci. Instrum.* **1994**, *65*(1), 7–12.

[14] G. Brindley. Identification of clay minerals by X-ray diffraction analysis. *Clay Clay Miner*. **1952**, *201*, 119–129. doi:10.1346/ccmn.1952.0010116.

[15] A. G. Attaelmanan. Reliability of a new X-ray analytical microscope in archaeological research. *J. Archaeol. Sci.* **2012**, *39*, 2552–2558.

[16] N. M. Suleman, I. A. Alagib, Quantitative and qualitative analysis of sand in Nafud desert at Zilfi province using ICP-MS spectroscopic technique. *J. Eng. Appl. Sci.* **2015**, *2*, 4–22.

[17] G. W. Morey, in *The Properties of Glass*. ACS monograph series No 124, 2nd edn (Ed: W. A. Hamor), Reinhold, New York, **1954**.

[18] A. Silverman. A chemist looks at glass. *Glass Ind.* **1953**, 428–433.